Activation of the Ano1 (TMEM16A) chloride channel by calcium is not mediated by calmodulin

Kuai Yu, Jinqiu Zhu, Zhiqiang Qu, Yuan-Yuan Cui, and H. Criss Hartzell

Department of Cell Biology, Emory University School of Medicine, Atlanta, GA 30322

The Ca^{2+}-activated Cl channel anoctamin-1 (Ano1; Tmem16A) plays a variety of physiological roles, including epithelial fluid secretion. Ano1 is activated by increases in intracellular Ca^{2+}, but there is uncertainty whether Ca^{2+} binds directly to Ano1 or whether phosphorylation or additional Ca^{2+}-binding subunits like calmodulin (CaM) are required. Here we show that CaM is not necessary for activation of Ano1 by Ca^{2+} for the following reasons. (a) Exogenous CaM has no effect on Ano1 currents in inside-out excised patches. (b) Overexpression of Ca^{2+}-insensitive mutants of CaM have no effect on Ano1 currents, whereas they eliminate the current mediated by the small-conductance Ca^{2+}-activated K^+ (SK2) channel. (c) Ano1 does not coimmunoprecipitate with CaM, whereas SK2 does. Furthermore, Ano1 binds very weakly to CaM in pull-down assays. (d) Ano1 is activated in excised patches by low concentrations of Ba^{2+}, which does not activate CaM. In addition, we conclude that reversible phosphorylation/dephosphorylation is not required for current activation by Ca^{2+} because the current can be repeatedly activated in excised patches in the absence of ATP or other high-energy compounds. Although Ano1 is blocked by the CaM inhibitor trifluoperazine (TFP), we propose that TFP inhibits the channel in a CaM-independent manner because TFP does not inhibit Ano1 when applied to the cytoplasmic side of excised patches. These experiments lead us to conclude that CaM is not required for activation of Ano1 by Ca^{2+}. Although CaM is not required for channel opening by Ca^{2+}, work of other investigators suggests that CaM may have effects in modulating the biophysical properties of the channel.

INTRODUCTION

In 2008, two members of the anoctamin superfamily, Ano1 and Ano2, were found to encode Ca^{2+}-activated Cl channels (CaCCs; Caputo et al., 2008; Schroeder et al., 2008; Yang et al., 2008). Since then, it has been shown that Ano1 (also known as Tmem16A) plays key roles in diverse physiological processes. Ano1 mediates Ca^{2+}-dependent fluid transport by a variety of epithelia (Ousingsawat et al., 2009), including salivary gland (Romanenko et al., 2010), airway (Rock et al., 2009), and bile duct (Dutta et al., 2011). Furthermore, Ano1 modulates mucin secretion by airway epithelium (Huang et al., 2012), regulates slow wave motility of the gut (Zhu et al., 2009; Huang et al., 2010; Cole, 2011; Dixon et al., 2012), participates in nociception by dorsal root ganglion neurons (Liu et al., 2010; Cho et al., 2012), regulates vascular and airway smooth muscle contraction (Davis et al., 2010; Manoury et al., 2010; Thomas-Gatewood et al., 2011; Bulley et al., 2012; Dixon et al., 2012; Huang et al., 2012; Davis et al., 2013), and may participate in the sperm acrosome reaction (Orta et al., 2012). Additionally, it has been suggested that Ano1 may impact cell proliferation and metastasis (Duvvuri et al., 2012; Mazzone et al., 2012; Ruiz et al., 2012; Britschgi et al., 2013).

Ano1 is activated by increases in cytosolic Ca^{2+} concentration with an EC_{50} in the low micromolar range (Kuruma and Hartzell, 2000; Xiao et al., 2011), but the gating mechanisms remain unresolved. Two possible mechanisms have been considered: (1) binding of Ca^{2+} directly to the channel or (2) binding of Ca^{2+} to a separate Ca^{2+} sensor protein such as calmodulin (CaM). We have proposed that Ano1 is regulated directly by Ca^{2+} binding to the channel because mutagenesis of two amino acids, E702 and E705, alters the Ca^{2+} sensitivity of the channel by several orders of magnitude (Yu et al., 2012). Mutation of homologous residues in the Ano1 paralogue Ano6 also dramatically decreases its Ca^{2+} sensitivity (Yang et al., 2012). Despite these dramatic results, their interpretation is ambiguous. The simplest interpretation is that these mutations alter a Ca^{2+}-binding site. However, allosteric consequences of mutations are difficult to exclude: for example, the mutation might alter the association of an accessory Ca^{2+} sensor. Furthermore, gating of the channel by direct Ca^{2+} binding has been questioned because the Ano1 sequence does not contain canonical Ca^{2+}-binding motifs and a sequence in the first intracellular loop resembling the "Ca^{2+} bowl" of the large conductance Ca^{2+}-activated K^+ channel does not appear to

be a principal Ca^{2+}-binding site (Ferrera et al., 2009; Xiao et al., 2011).

Several studies have implicated a role of CaM in regulating Ano1 currents. Tian et al. (2011) have reported that trifluoperazine (TFP) or J-8, classical inhibitors of CaM, decreases activation of Ano1(*abc*) by Ca^{2+}. They identified an alternatively spliced segment (termed segment *b*) in Ano1 as a CaM-binding site. However, the conclusion that CaM is required for Ano1 activation is contradicted by the robust Ca^{2+}-dependent activation of the Ano1(*ac*) splice variant that lacks the *b* segment (Xiao et al., 2011). Recently, Jung et al. (2013) reported that CaM binds in a Ca^{2+}-dependent manner to two different sites in Ano1(*ac*): one site (CBM1) is immediately N-terminal to the putative first transmembrane segment, and the other is immediately N-terminal to the putative seventh transmembrane segment (CBM2). Jung et al. (2013) show that Ca^{2+}-CaM binding increases the relative Cl^-:HCO_3^- permeability of the channel. While our paper was in review, two other papers appeared on the role of CaM in Ano1 regulation. Vocke et al. (2013) report that TFP and J-8 do not inhibit Ano1 currents (in contrast to Tian et al. [2011]), but they show that purified peptides corresponding to CBM1 bind to CaM and that overexpression of certain CaM mutants reduces Ano1 current density. Finally, Terashima et al. (2013) have purified recombinant Ano1 expressed in Sf9 cells and find that the purified Ano1 protein reconstitutes Ca-activated Cl channels in liposomes without the presence of CaM. Furthermore, they were unable to find evidence that CaM bound to purified Ano1 by a variety of assays with the purified proteins.

In light of these conflicting results, we wanted to clarify whether activation of Ano1 by Ca^{2+} involves CaM. There are at least six ways by which CaM can regulate its effectors (Chin and Means, 2000). Class A effectors bind essentially irreversibly to CaM irrespective of Ca^{2+} concentration. In these effectors, CaM is a "constitutive" subunit of the protein complex. The effector is activated allosterically by Ca^{2+} binding to the tethered CaM. This mode of CaM signaling has been demonstrated to be responsible for activation of the small-conductance K^+ (SK) channel by Ca^{2+} (Xia et al., 1998) and for Ca^{2+}-dependent facilitation and inactivation of voltage-gated Ca_V1 and Ca_V2 channels (Erickson et al., 2001). Regulation of class A effectors by CaM is relatively insensitive to pharmacological inhibitors like TFP. Class B effectors also bind Ca^{2+}-free CaM (apo-CaM), but Ca^{2+} binding stimulates CaM dissociation from the effector. Class C effectors bind to CaM with low affinity at low Ca^{2+} concentrations (<2 mol Ca^{2+}/mol CaM), whereas at high Ca^{2+} concentrations, class C effectors form a high-affinity complex with Ca^{2+}-CaM. Class D and E effectors do not bind apo-CaM, but bind Ca^{2+}-CaM reversibly and are inhibited or activated, respectively, by Ca^{2+}-CaM binding. Class F effectors are activated by phosphorylation, but

phosphorylation is promoted by CaM binding to the effector. The results of Tian et al. (2011) and Jung et al. (2013) are consistent with Ano1 being a class E effector because CaM binding is only observed in the presence of Ca^{2+} and the activation of the channel by Ca^{2+} is inhibited by TFP. However, the data we present here are more consistent with the conclusion that Ano1 activation by Ca^{2+} occurs by direct binding of Ca^{2+} to Ano1 and that the activation of Ano1 by Ca^{2+} is not mediated by CaM.

MATERIALS AND METHODS

Electrophysiology

mAno1(*ac*) tagged with EGFP at the C terminus was provided by U. Oh (Seoul National University, Seoul, South Korea). Unless indicated otherwise, experiments used mouse Ano1 (mAno1). Both the *ac* (UniProt accession no. Q8BHY3) and *abc* (QGEGRRKD-SALLSKRRKCGKYG inserted after position 266 in Ano1*ac*) splice variants were used. SK2 cDNA was provided by J. Adelman (Vollum Institute, Portland, OR). cDNA was transfected into HEK293 cells (0.1–1 µg total DNA per 3.5-cm plate) using Fugene-6 (Roche). Single cells identified by EGFP fluorescence were used within 72 h. Transfected HEK293 cells were recorded using conventional whole-cell or excised inside-out patch-clamp techniques with an EPC-7 amplifier (HEKA). Fire-polished borosilicate glass patch pipettes were 3–5 MΩ. Experiments were conducted at room temperature (20–24°C). Because liquid junction potentials were small (<2 mV), no correction was made. The zero Ca^{2+} intracellular solution contained (mM): 146 CsCl, 2 $MgCl_2$, 5 EGTA, 10 sucrose, and 10 HEPES, pH 7.3, adjusted with NMDG. The high Ca^{2+} pipette solution contained 5 mM Ca^{2+}-EGTA (free Ca^{2+} ∼20 µM) instead of EGTA. Solutions with various free Ca^{2+} concentrations were made by mixing $CaCl_2$ with EGTA or hydroxyethyl-EDTA (HEDTA), as calculated by the MaxChelator Program (Patton et al., 2004), and the free Ca^{2+} concentration was verified using a Ca^{2+} ion–selective electrode. In experiments with SK2 channels, 146 mM KCl replaced equimolar CsCl in the high-Ca pipette solution. Ba^{2+}-containing solutions were made by adding $BaCl_2$ and 1 mM EGTA to Chelex-100–treated zero-Ca solution to generate a free calculated Ba^{2+} concentration using the MaxChelator program. EGTA affinity is much lower for Ba^{2+} than for Ca^{2+}. The standard extracellular solution contained (mM): 140 NaCl, 5 KCl, 2 $CaCl_2$, 1 $MgCl_2$, 15 glucose, and 10 HEPES, pH 7.4 with NaOH. For recordings of SK2 currents, 140 mM KCl replaced equimolar NaCl in the extracellular solution. Purified CaM (EMD Millipore) was added to recording solutions from a stock solution of Ca^{2+}-CaM. Osmolarity was adjusted with sucrose to 303 mOsm for all solutions.

Photolysis of caged Ca^{2+}

Cells were placed on the stage of an Axiovert inverted microscope (Carl Zeiss). The microscope condenser assembly was replaced with a 100-W xenon model JML flash lamp (Rapp Optoelektronik GmbH) filtered by a UG11 filter (∼300–400 nm band pass) focused onto the recording chamber with an 18-mm-focal-length lens, which produced a 4-mm-diameter spot of illumination (Rapp and Güth, 1988; Frace et al., 1993). Flash intensity was adjusted by changing the condenser charging voltage. We typically used 4-mJ/mm^2 flashes. The duration of the flash was <1 ms. Cells were loaded with caged Ca^{2+}, *o*-nitrophenyl–EGTA (NP-EGTA; Invitrogen; Ellis-Davies and Kaplan, 1994), from the patch pipette. The pipette solution contained (mM) 2 NP-EGTA, 136 CsCl, 1.5 $CaCl_2$, 1 $MgCl_2$, and 25 HEPES-NMDG, pH 7.5. Before photolysis, the free Ca^{2+} concentration was calculated to be 80 nM and the Ano1 current was typically l ≤ 100 pA in amplitude.

Rapid perfusion

The fast application of Ca^{2+} to excised inside-out patches was performed using double-barreled theta tubing (1.5 mm o.d.; Sutter Instrument) with a tip diameter of ~50 µm attached to a Piezo bimorph on a micromanipulator (Xiao et al., 2011; Yu et al., 2012). One barrel was filled with standard zero-[Ca^{2+}] solution, and the other barrel was filled with intracellular solution containing Ca^{2+} (or Ba^{2+} for experiments in Fig. 7). Excised patches were positioned at the opening of one barrel of the theta tubing, and the barrel flooding the patch was switched by applying ~100 V to the Piezo bimorph. The time course of solution exchange across the laminar flow interface was estimated by liquid junction potential measurements to be <5 ms.

Immunoprecipitation and pull-down experiments

For immunoprecipitation experiments in Fig. 5, HEK293 cells were transfected with Ano1-EGFP or SK2 plus CaM tagged on the N terminus with FLAG and myc (provided by R. Dolmetsch and C.Y. Park, Stanford University, Stanford, CA; Mullins et al., 2009). 2–3 d after transfection, one set of dishes was treated with 10 µM ionomycin for 4 min in Hanks BSS to elevate intracellular Ca^{2+}, and the other set was untreated. The untreated cells were lysed in Ca^{2+}-free Buffer A (mM): 150 NaCl, 10 HEPES, 1 EGTA, and 0.1 $MgCl_2$, pH 7.4, containing 0.5% Triton X-100 and Complete Anti-protease (Roche). Ionomycin-treated cells were lysed in Ca^{2+}-containing Buffer A that lacked EGTA and had 1 mM of added $CaCl_2$. For ionomycin-treated cells, Ca^{2+} was present in all subsequent steps. The clarified supernates were applied to 20 µl anti-FLAG antibody–coated Dynal magnetic beads and incubated for 2 h. The beads were washed three times with 300 µl Buffer A (with EGTA or Ca^{2+}, as appropriate). Proteins were solubilized from the beads with 50 µl Laemmli SDS sample buffer, electrophoresed on 4–20% acrylamide SDS-PAGE gels, and subjected to Western blotting using anti-Ano1 (Ano1-EGFP = 150 kD) and anti-myc (CaM = 17 kD).

For pull-down experiments in Fig. 6, HEK293 cells were transfected with human Ano1 (hAno1; provided by M.G. Lee, Seoul National University; Jung et al., 2013), mAno1-FLAG(3X), or CaMKIIα-Venus (plasmid #29427; Addgene; Thaler et al., 2009). HEK cell lysate (300 µl containing 750 µg protein) was mixed with 600 µl of binding buffer (with EGTA or Ca^{2+}) and 120 µl CaM-GST–Sepharose beads containing 450 µg CaM as described by Jung et al. (2013). After an overnight incubation at 4°C, bead complexes were washed five times. Bound protein was eluted with 60 µl SDS sample buffer and immunoblotted with antibodies against hAno1 (Dog1.1; gift of R. West, Stanford University), anti-flag (M2 monoclonal; Sigma-Aldrich), or anti-CaMKII (Sigma-Aldrich).

Analysis of data

Electrophysiological traces were analyzed with Clampfit 9 (Molecular Devices). Data are presented as mean ± SEM. Statistical difference between means was evaluated by two-tailed t test. Statistical significance was assumed at $P < 0.05$. Immunoblots were scanned using an Epson Perfection V700 desktop scanner and analyzed using myImageAnalysis version 1.1 software (Thermo Fisher Scientific).

RESULTS

Characterization of Ano1 activation by Ca^{2+}

As a first step to exploring the mechanism of Ano1 activation by Ca^{2+}, we first wanted to know the speed of Ano1 activation by Ca^{2+}. To determine the rate of Ano1 activation by Ca^{2+}, we recorded Ano1 currents in response to photolysis of caged Ca^{2+} (NP-EGTA) with whole-cell patch-clamp using solutions that lacked ATP to minimize phosphorylation. With a 4-mJ/mm^2 intensity UV flash, Ano1 currents activated very rapidly. Fitting the rising phase of the current to the sum of two exponentials revealed that the major component of the current increased with a time constant $\tau = 1.2 \pm 0.1$ ms (see Fig. 1 legend for details). The precise instant that the current began to increase was obscured by the flash artifact, but invariably the current had increased significantly above baseline by the end of the 600-µs flash (Fig.1, A and B). Some of the latency may be explained by the rate of Ca^{2+} release from NP-EGTA, which is 6.8×10^4/s as measured with a 180-mJ/mm^2 laser flash at the optimal excitation wavelength of 357 nm (Ellis-Davies et al., 1996;
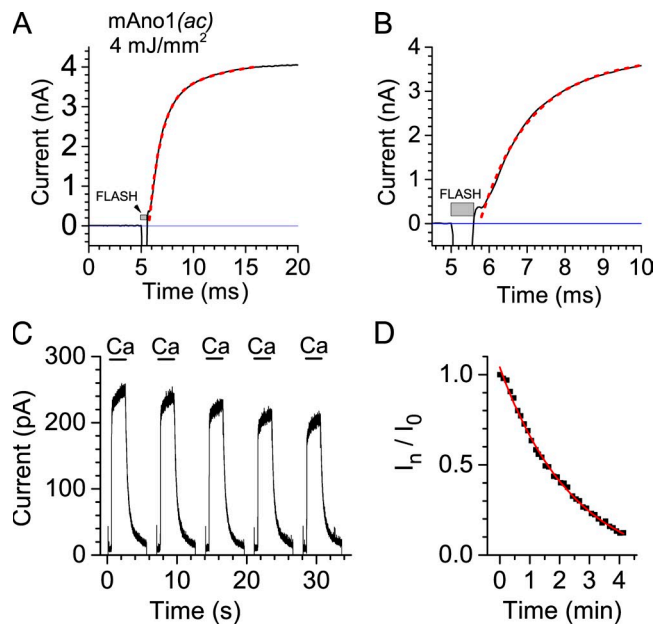

Figure 1. Activation of Ano1 currents by Ca^{2+} in the absence of ATP or exogenous CaM. (A) Kinetics of Ano1 current activation in response to photolysis of caged Ca^{2+} in whole-cell recording. Cells were whole-cell patch-clamped at a holding potential of 100 mV with an internal solution lacking ATP and containing NP-EGTA loaded with Ca^{2+}. Ca^{2+} was released by photolysis using a 4-mJ/mm^2 flash from a flash lamp at the arrow as indicated. For a period of 10 ms (5.8–15.8 ms) starting at the time of current onset, the activation of the mean of five currents (black line) was fitted (red line) to the equation $I_t = I_0 + I_1 \times (1 - e^{-t/\tau 1}) + I_2 \times (1 - e^{-t/\tau 2})$, where t is time in ms, $I_0 = 0.15$ nA, $I_1 = 3.14$ nA, $I_2 = 1.11$ nA, $\tau_1 = 1.18$ ms, $\tau_2 = 9.8$ ms; $r^2 = 0.999$. A fit to a single exponential for the period 5.8–11.3 ms was slightly less good, ($\tau = 1.4$ ms) $r^2 = 0.9955$. (B) The onset of the current shown in A is shown on an expanded time scale with the double exponential fit. (C) Repeated activation of Ano1 current by Ca^{2+} in an inside-out excised patch in the absence of added ATP. An inside-out excised patch at a holding potential of 100 mV was switched between 0 and 20 µM Ca^{2+} as indicated. The solution was changed by moving a theta tubing perfusion pipe mounted on a Piezo bimorph. The solution change occurred in <5 ms (Perez-Cornejo et al., 2012). (D) The amplitude of the Ano1 current evoked by each Ca^{2+} pulse (I_n) was normalized to the amplitude of the first response (I_0; I_n/I_0). This graph shows the entire experiment of C. C shows pulses 21–25 (2.4–2.9 min).

Ellis-Davies and Barsotti, 2006). Because the energy density of our flash was >40-fold smaller, the rate of Ca^{2+} release is likely slower. This rapid activation rate is comparable with rates reported for the class A CaM effector SK channel (Xia et al., 1998) and ligand-gated ion channels such as the nicotinic ACh receptor (Lester et al., 1980). The activation rate is slower than would be expected if Ano1 was gated open by Ca^{2+}-stimulated phosphorylation. Although protein kinases can operate at rates as high as 20/s (Adams and Taylor, 1992), Ca^{2+} activates the Ano1 current at a rate of >800/s ($\tau = 1.2 \pm 0.1$ ms) without added ATP.

The observation that the Ano1 current is activated in the absence of added ATP (Fig. 1) suggests that Ca^{2+} does not activate the channel by stimulating protein phosphorylation. However, in whole-cell recording, phosphorylation might occur because the cell may produce ATP endogenously by glycolysis or oxidative phosphorylation. Furthermore, activation of Ano1 could hypothetically be explained by Ca^{2+}-dependent dephosphorylation of a previously phosphorylated channel. To test these possibilities, we examined activation of the Ano1 current in excised inside-out patches where cytosolic ATP could be rigorously controlled. Ano1 current was activated by Ca^{2+} in excised patches even when the cytosolic face of the excised patch was perfused with intracellular solution lacking any high-energy substrates (ATP, GTP, and glucose). Furthermore, the current could be turned on and off repeatedly by switching between Ca^{2+}-free and Ca^{2+}-containing solutions (Fig. 1 C). This result eliminates reversible dephosphorylation/phosphorylation as the triggering event in Ca^{2+}-dependent opening and closing of the Ano1 channel.

The result in Fig. 1 C places certain constraints on an activation mechanism that involves gating by Ca^{2+}-CaM. Because the current can be activated many times by repeatedly switching between Ca^{2+}-containing and Ca^{2+}-free solutions, the Ca^{2+} sensor must be effectively anchored to the excised patch so that it does not freely diffuse away between Ca^{2+} applications. In other words, it is unlikely that Ano1 is a class E CaM effector where Ca^{2+}-CaM reversibly binds to the channel to open it (see Discussion for a more thorough discussion of CaM dissociation and diffusion rates). These experiments provide evidence that the activation of Ano1 is membrane delimited: freely diffusible, reversibly bound soluble proteins are unlikely to be necessary for activation of the current by Ca^{2+}.

Although the Ano1 current can be repeatedly activated in excised patches, the amplitude of the current runs down with time. In the example of Fig. 1 C, the current decreased exponentially with $\tau = 2.45$ min (Fig. 1 D). The rundown could be explained by various mechanisms, but one possibility would be a slow loss of CaM from the patch. Rundown was quantified by exposing excised patches to cytosolic solution containing different

concentrations of free Ca^{2+}. With 1.4 or 3.4 µM free Ca^{2+} in the solution bathing the cytosolic face of the patch, current rundown was relatively slow and incomplete during the recording (Fig. 2). With these low micromolar concentrations of Ca^{2+}, Ano1 current decreased $\sim$25% over a period of 5 min and then stabilized (Fig. 2 A, open symbols). Higher concentrations of Ca^{2+} (>10 µM) accelerated current rundown. With 20 µM Ca^{2+}, the current ran down $\sim$55% in 5 min, whereas with 74 µM Ca^{2+}, the current ran down >95% in <5 min (Fig. 2, A and B). Current rundown could not be reversed by washing the patch with zero-Ca^{2+} solution for several minutes before switching back to Ca^{2+}-containing solution. The finding that current rundown depends on the concentration of cytosolic Ca^{2+} and that rundown is irreversible is consistent with rundown being caused by CaM loss from the patch. In the next section this hypothesis is tested experimentally.

Exogenous CaM has no effect on Ano1 currents
If the rundown of current is caused by loss of CaM, one would expect that addition of exogenous CaM to the cytosolic solution would restore the current. A large number of experiments were performed applying purified brain CaM at concentrations ranging from 1 to 25 µM to the cytosolic side of the patch. However, CaM application never reversed or obviously slowed rundown. Several
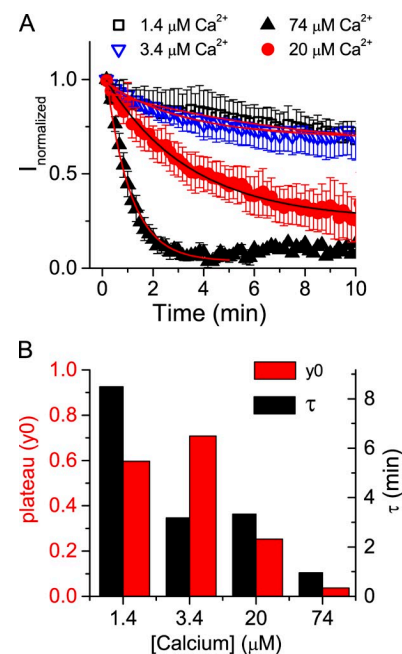

Figure 2. Rundown of Ano1 current in excised patches. (A) Excised patches were pulled from cells expressing Ano1(*ac*) and exposed to internal solution containing 1.38, 3.36, 20, and 74.35 µM Ca^{2+}. Current amplitudes at 100 mV are plotted versus time in Ca^{2+}-containing solution ($n = 3$–10). The data were fitted to an exponential $I_{(t)} = y_0 + A \times e^{-t/\tau}$, where t is time in ms and y_0 is the plateau level of rundown. Error bars are ±SEM. (B) The time constant of rundown (τ) and the extent of rundown expressed as y_0 for the data in A are plotted versus free Ca^{2+} in the cytosolic solution.

examples are shown in Fig. 3. Addition of 10 µM to the cytosolic solution had no effect on currents carried by Ano1(ac) (Fig. 3 A) or Ano1(abc) (Fig. 3 B) in inside-out excised patches. The effect of CaM was quantified by measuring rundown for 1 min before CaM application and 1 min during CaM application (Fig. 3 C). With both isoforms, rundown occurred at statistically the same rates whether CaM was present or not. One possible explanation for the absence of effect of CaM is that its association with Ano1 is very slow and that a 1-min exposure is insufficient time for CaM to bind. However, applications of 10 µM CaM for >8 min had no effect on the rate or extent of rundown (Fig. 3 A, inset). Exponential fits of the rundown from the time of switch to CaM-containing or control solution were control: $\tau = 2.9 \pm 0.4$ min, $y_0 = 0.51 \pm 0.02$; and CaM: $\tau = 3.6 \pm 0.7$ min, $y_0 = 0.49 \pm 0.04$, where y_0 is the level of the current remaining after rundown has completed compared with the initial current. After the current had run down completely in solutions containing high Ca^{2+} concentrations, addition of CaM did not restore the current (Fig. 3 D). The finding that exogenous Ca^{2+}-CaM had no effect raised the question of whether exogenous apo-CaM would have any effect. To test the effect of apo-CaM, the patch was first activated

with 20 µM Ca^{2+} and then the solution was replaced with a zero-Ca^{2+} solution containing 25 µM apo-CaM that had been dialyzed against the zero-Ca^{2+} EGTA solution (Fig. 3 E). Current amplitudes in zero-Ca^{2+} solution and in zero-Ca^{2+} plus apo-CaM were identical ($n = 4$). Subsequent exposure of the patch to 20 µM Ca^{2+} evoked a current similar in amplitude to that expected if rundown had continued at a constant rate during apo-CaM exposure. Subsequent addition of 25 µM Ca^{2+}-CaM had no effect (Fig. 3 E). The rate of current rundown was virtually identical in 20 µM Ca^{2+} in the presence and absence of 25 µM CaM and before or after exposure to apo-CaM (Fig. 3 F). The data indicate that rundown is not caused by the loss of CaM from the patch and that Ano1 is not a class E CaM effector.

Several caveats should be mentioned. Rundown may be a process unrelated to Ca-dependent gating, for example, a process involving loss or modification of requisite components including protein subunits or lipids. If that is the case, one would not expect CaM to reverse the rundown process even if CaM is required for activation of the current by Ca^{2+}. The present experiments also would not exclude a mechanism in which rundown is caused by a loss of CaM from excised patches but the
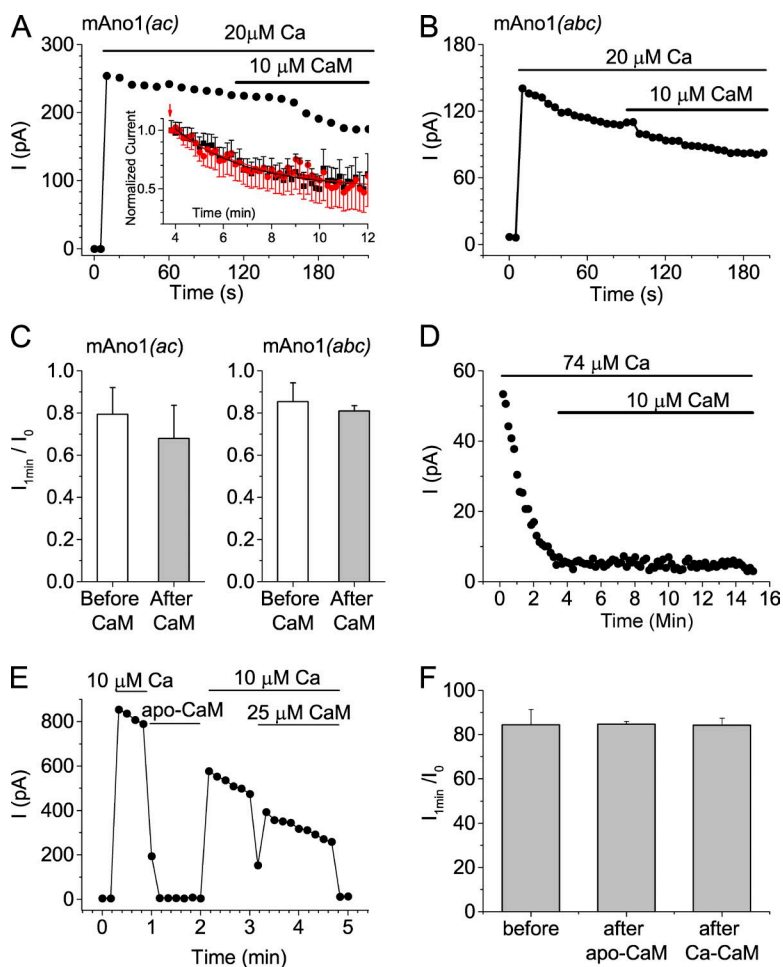

Figure 3. Exogenous CaM has no effect on Ano1 current in inside-out excised patches. (A and B) Excised patches were pulled from cells expressing Ano1(ac) (A) and Ano1(abc) (B) and exposed to 20 µM Ca^{2+} with or without 10 µM CaM as indicated at 100-mV holding potential. Application of CaM has no effect ($n = 5$–10). The inset in A compares rundown in excised patches not exposed to CaM (black) and patches exposed to 10 µM CaM (red) for 8 min. (C) Rundown was quantified before and during exposure to CaM as $I_{end}/I_{initial}$, where I_{end} is the current amplitude at the end and $I_{initial}$ is the current amplitude at the start of a 1-min period. (D) Rundown of Ano1(abc) in response to 74.35 µM Ca^{2+} was not rescued by 10 µM CaM. (E and F) Ano1 rundown in the presence of 10 µM Ca is not affected by addition of 25 µM apo-CaM in the absence of Ca^{2+} or Ca^{2+}-CaM. Rundown was quantified as in C. Error bars are ±SEM.

conditions required for rebinding of exogenous CaM are suboptimal or very slow.

Effects of Ca²⁺-insensitive CaM on Ano1 currents

Class A CaM effectors, such as the small conductance K⁺ channel SK2 (Xia et al., 1998; Maylie et al., 2004), have CaM tethered to the pore-forming polypeptide as an integral subunit: both apo-CaM and Ca²⁺-CaM are tightly bound. It has been shown that overexpression of CaM mutants defective in Ca²⁺ binding (Geiser et al., 1991) can compete for native CaM and eliminate effects of Ca²⁺ on class A effectors, including SK2 (Xia et al., 1998) and Ca$_V$ channels (Peterson et al., 1999). Ca²⁺-insensitive CaM generated by mutagenesis of aspartate to alanine in the second, third, and fourth EF hands (CaM$_{2,3,4}$) or all four EF hands (CaM$_{1,2,3,4}$) greatly reduces SK2 currents (Xia et al., 1998). Fig. 4 shows that currents recorded from Ano1 coexpressed with wild-type CaM or CaM$_{1,2,3,4}$ had the same mean amplitudes and exhibited similar voltage and time dependence and current-voltage relationships (Fig. 4, A and B). CaM$_{2,3,4}$ had no effect on the outward current but produced a small increase in the

inward current at potentials negative to -60 mV. Control experiments performed on the same day with the SK2 channel showed that both of the mutant CaM constructs completely eliminated SK currents (Fig. 4, D–F). From these experiments, we conclude that CaM is not a constitutively bound subunit of the Ano1 channel necessary for Ano1 activation by Ca²⁺. However, we cannot exclude the possibility that the mutant CaMs are incapable of binding to Ano1 even though they are capable of binding to SK2.

Interaction of Ano1 with CaM is weak

Analysis of the mouse Ano1 sequence by the Calmodulin Target Database identifies two potential CaM-binding sites with scores >5 (out of a possible 10). Neither of these sites conform exactly to established CaM-binding sequences, but they resemble CaM-binding "1-8-14 motifs." 1-8-14 motifs are characterized by bulky hydrophobic amino acids at positions 1, 8, and 14 and are typically found in class E effectors that bind reversibly to Ca²⁺-CaM (Rhoads and Friedberg, 1997). The first site (²⁷⁷<u>A</u>LLSKRRKCGKYG<u>I</u>²⁹⁰, numbering based on the *abc*
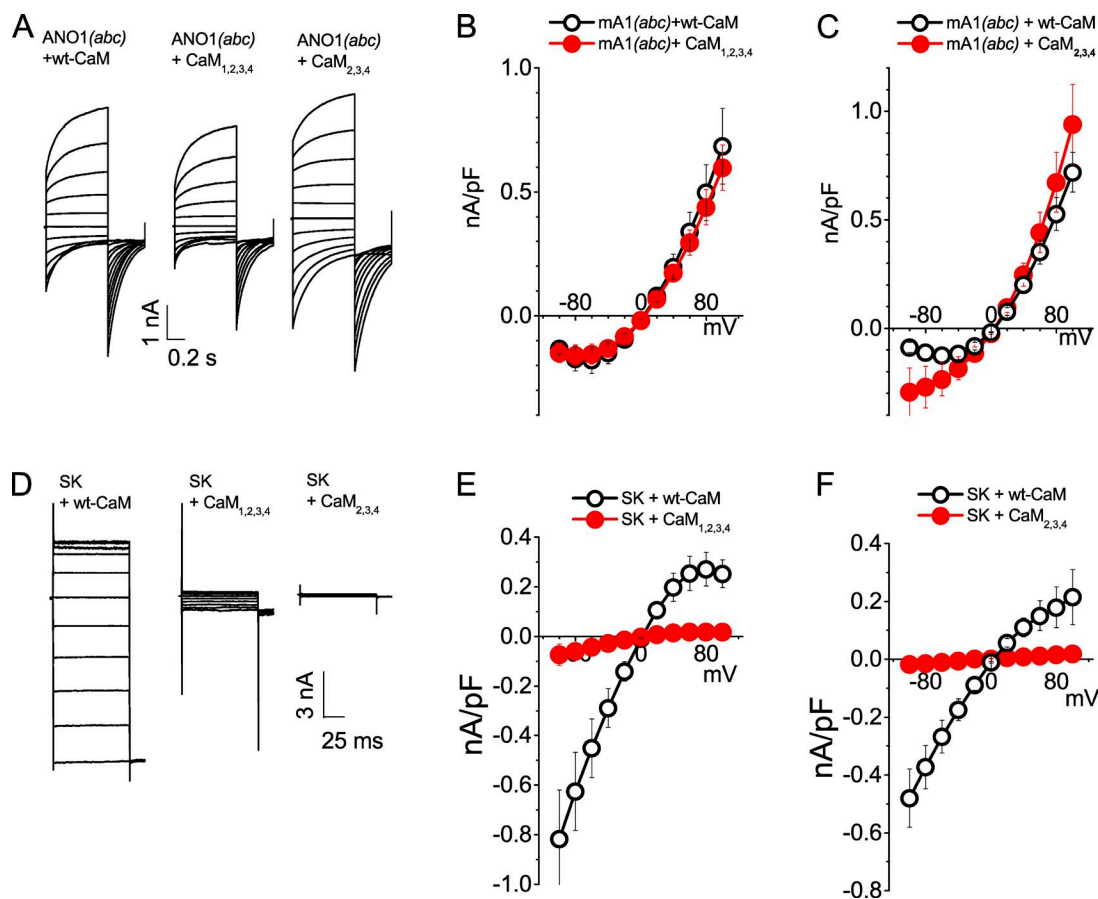

Figure 4. Overexpression of dominant-negative CaM$_{1,2,3,4}$ or CaM$_{2,3,4}$ has no effect on Ano1 current amplitude or kinetics but suppresses SK2 currents. (A and D) Current traces from cells expressing mAno1(*abc*) (A) or SK2 (D) with or without CaM$_{1,2,3,4}$ or CaM$_{2,3,4}$. (B, C, E, and F) Steady-state current-voltage relationships for Ano1(*abc*) (B and C) or SK2 (E and F) coexpressed with CaM$_{1,2,3,4}$ (B and E) or CaM$_{2,3,4}$ (C and F; $n = 5$–10). To test whether the effect of CaM might vary with [Ca²⁺], experiments with CaM$_{1,2,3,4}$ used 20 µM free Ca²⁺ and experiments with CaM$_{2,3,4}$, used 1 µM Ca²⁺. Error bars are ±SEM.

isoform) overlaps with the *b* splice segment and is not present in the Ano1*ac* isoform (Ferrera et al., 2009; Tian et al., 2011). The second site (³³⁹IDLVRKYFGEKVGL³⁵²; CBM1 [Jung et al., 2013]) is located immediately N-terminal to the putative first transmembrane segment and is present in both *ac* and *abc* isoforms.

To determine whether CaM binds to either isoform of Ano1, we performed immunoprecipitation experiments on HEK293 cells cotransfected with CaM (FLAG and myc tagged) plus Ano1(*ac*), Ano1(*abc*), or SK2. To test whether the association of CaM with Ano1 is Ca^{2+} dependent, immunoprecipitation was performed on cells with basal cytosolic Ca^{2+} (presumed to be ~100 nM) and on cells in which Ca^{2+} was elevated with ionomycin before lysis. After lysis in Ca^{2+}-free or Ca^{2+}-containing buffer, respectively, CaM was immunoprecipitated using magnetic beads coated with anti-Flag antibody, and the immunoprecipitate was immunoblotted for the presence of Ano1, SK2, and CaM (Fig. 5). The immunoprecipitate from cells expressing CaM plus SK2 contained large amounts of SK2 (which appeared as monomers, dimers, and higher-order oligomers on the gel). In contrast, in cells expressing CaM plus either mAno1(*ac*) or mAno1(*abc*), there was no Ano1 protein in the immunoprecipitate regardless of whether the lysate was obtained from cells with resting Ca^{2+} or elevated Ca^{2+}. The positive control with the SK2 channel validates the method. The absence of Ano1 coimmunoprecipitation with CaM supports our physiological data that CaM binding is not required for activation of the current by Ca^{2+}.

The conclusion from Fig. 5 is different from that recently reported by Jung et al. (2013). These authors demonstrate a physical interaction between human Ano1(*ac*) and CaM-GST in a pull-down assay. Therefore, we tested the ability of CaM-GST beads to pull down mouse Ano1(*ac*) human Ano1(*ac*) from lysates of transfected HEK cells (Fig. 6). First, we performed a positive control to evaluate this method. We prepared lysates from HEK cells overexpressing CaMKIIα and examined the ability of CaM-GST to capture CaMKIIα from the lysate (Fig. 6 A). As estimated from densitometric scans of band intensity, ~10 times more CaMKIIα bound to CaM-GST beads in the presence than in the absence of Ca^{2+} (Fig. 6 E). To estimate the fraction of CaMKIIα in the lysate that was captured by the beads, we compared the intensity of the CaMKIIα band bound to the beads to various dilutions of the lysate (lanes 1–4). Densitometric scans show that virtually all of the CaMKIIα in the lysate was captured by the beads (Fig. 6 E).

Consistent with the results of Jung et al. (2013), we found that two times more hAno1(*ac*) bound to CaM-GST in the presence of Ca^{2+} than in the absence of Ca^{2+} (Fig. 6 C). A similar result was obtained with mAno1(*ac*) (Fig. 6 B). To evaluate the fraction of Ano1 that bound to the CaM-GST beads, we compared the amount of Ano1 that bound to the CaM-GST beads relative to the amount of Ano1 present in the lysate. Different amounts of lysate were loaded onto the gel, and the densitometric area of the bands was measured. Less than 1% of either hAno1 (*ac*) or mAno1(*ac*) in the lysate bound to the CaM-GST
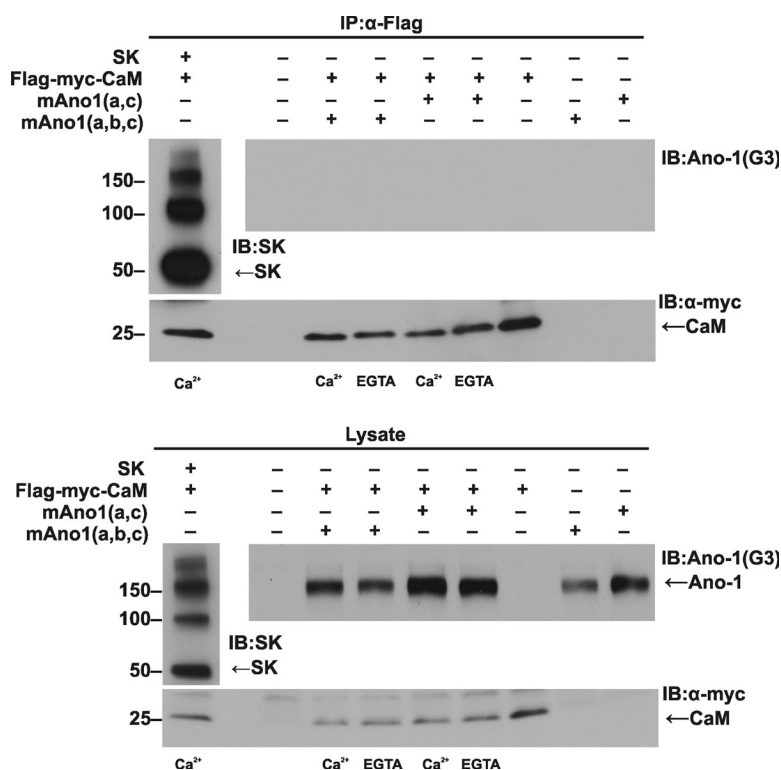

Figure 5. Immunoprecipitation of CaM does not coimmunoprecipitate Ano1 but does coimmunoprecipitate SK2. Flag- and myc-tagged CaM was coexpressed with mAno1(*abc*), mAno1(*ac*), or SK2 in HEK 293 cells. Cells were lysed in medium containing EGTA or medium containing Ca^{2+} after treatment with ionomycin to elevate cytosolic Ca^{2+}. CaM was immunoprecipitated with anti-Flag antibody. The immunoprecipitate (IP) was subjected to Western blot and probed with antibody to Ano1, SK2, or myc (for CaM). (top) Immunoprecipitate. (bottom) Total lysate. Molecular mass is indicated in kilodaltons. IB, immunoblot.

beads (Fig. 6, E and F). As shown above, this compares with ~100% of CaMKIIα that binds. These results show that although CaM may bind to Ano1(ac), the binding is less robust than the binding to CaMKIIα. This could be explained if CaM has a much lower affinity for Ano1 than for CaMKIIα or if the stoichiometry of CaM binding to Ano1 is low, for example if CaM binds only to Ano1 in a certain state (conformational, posttranslational modification, etc.) that is poorly represented in the Ano1 preparation we have used. Alternative explanations are considered in the Discussion.

Activation of Ano1 by Ba^{2+}

Chao et al. (1984) have shown that Ba^{2+} has an extremely low affinity for CaM. The affinity of divalent cation binding to CaM exhibits the sequence $Ca^{2+} > Sr^{2+} \gg Mg^{2+} > Be^{2+} > Ba^{2+}$. Furthermore, the maximal effect of Ba^{2+} on CaM conformation as measured by tyrosine fluorescence was <2% as large as that produced by Ca^{2+}. As an additional test of the involvement of CaM, we tested the effect of Ba^{2+} on Ano1 currents. In both whole-cell recording and in inside-out excised patches, >10 µM Ba^{2+}

activated large Ano1 currents (Fig. 7). In whole-cell recording, the EC_{50} was estimated to be 25 µM Ba^{2+} (Fig. 7 B). To estimate Ba^{2+} affinity in inside-out excised patches, we corrected for variations in the size of the patch and number of channels contained in different patches by normalizing the currents to the maximum Ano1 current activated by 1 mM Ba^{2+} in each patch. Furthermore, to correct for rundown, patches were exposed to 1 mM Ba^{2+}, then the test Ba^{2+} concentration, and then again 1 mM Ba^{2+}, each for ~5 s. The response to the test concentration was then expressed as a fraction of the mean of the responses to the two 1 mM Ba^{2+} applications. These experiments show that the EC_{50} for Ba^{2+} in excised patches is very similar to whole-cell recording, 14 µM. The differences may reflect rundown that occurs in whole-cell recording before complete equilibration of the pipette solution with the cytoplasm.

The EC_{50} for Ba^{2+} is ~50-fold larger than the EC_{50} we have estimated for Ca^{2+} (Xiao et al., 2011). Additional support for the conclusion that Ca^{2+} does not activate Ano1 by binding to CaM is the finding that Mg^{2+} does not activate Ano1, despite the fact that the affinity of
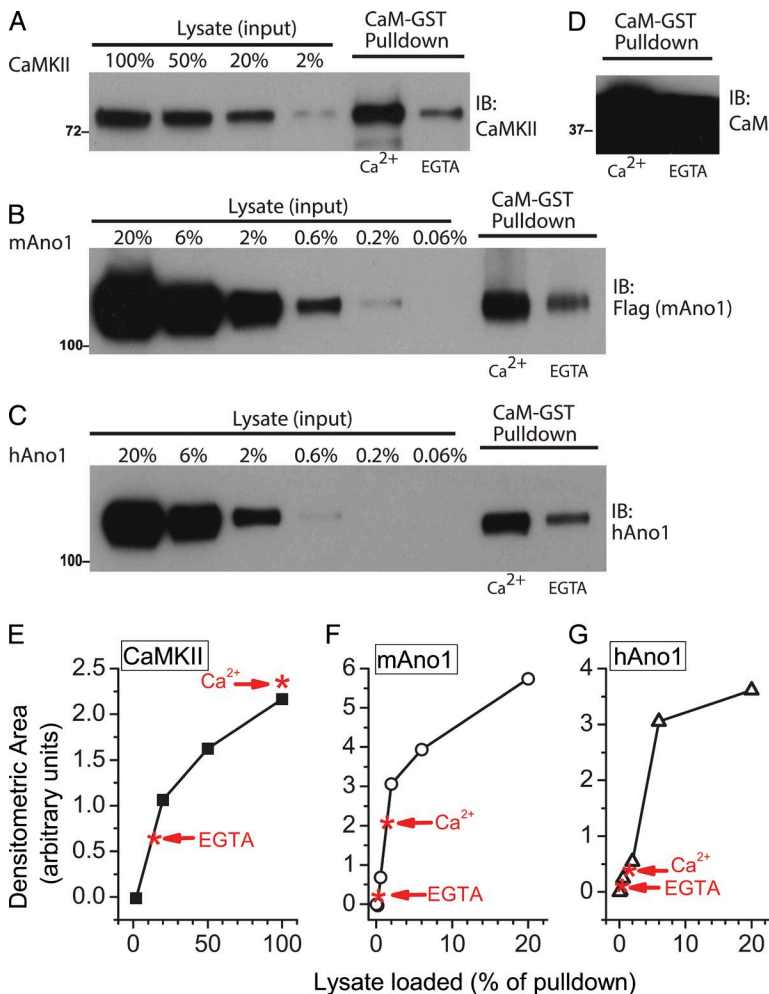

Figure 6. CaMKIIα is pulled down more efficiently than Ano1 by CaM-GST. (A–C) Lysates from HEK cells overexpressing CaMKIIα (A), mAno1(ac) (B), or hAno1(ac) (C) were incubated with CaM-GST–Sepharose beads. Lysates were prepared in buffer containing 100 µM Ca^{2+} or EGTA as indicated. Proteins that bound to the beads were detected by immunoblot (IB) with antibodies to hAno1, Flag (for mAno1), or CaMKIIα. Pull-down lanes (two right-most lanes in A–C) contain 1/8 of the protein eluted from the beads. The lysate lanes (left) contain different amounts of lysate expressed as a percentage of the amount of pull-down eluate loaded (for example, 100% represents 1/8 of total lysate). (D) Blot of CaM eluted from beads under same conditions as A–C to show large excess of CaM. Molecular mass is indicated in kilodaltons. (E–G) Quantification of data in A–C. Immunoblots were analyzed by densitometry, and the intensity of each band is expressed as area in relative units. Black lines plot the intensities of different amounts of lysate. Red asterisks indicate the intensity of the pull-down bands in the presence (Ca^{2+}) and absence of Ca^{2+} (EGTA). (E) CaMKIIα. (F) mAno1(ac). (G) hAno1(ac).

CaM for Mg^{2+} is higher than for Ba^{2+} (Chao et al., 1984). 2 mM Mg^{2+} is present in our zero-Ca^{2+} intracellular solution, but it does not activate Ano1.

TFP does not block Ano1 from the cytoplasmic side

Another piece of evidence that has been offered to support the hypothesis that Ca^{2+} activates Ano1 by binding to CaM is the finding that CaM antagonists such as TFP suppress the Ano1 current (Tian et al., 2011), although Vocke et al. (2013) found that TFP did not inhibit Ano1. TFP is notoriously nonspecific. For example, TFP inhibits the gating of the large-conductance Ca^{2+}-activated K^+ channel (BK channel) with an apparent K_d of 1.4 µM by a mechanism independent of CaM (McCann and Welsh,

1987; Ikemoto et al., 1992), and TFP is known to disrupt the physical properties of phospholipid monolayers at a low molar ratio of TFP to lipid (Hidalgo et al., 2004). Therefore, we wanted to examine the mechanisms of TFP action on Ano1. Fig. 8 (A–C) confirms another report (Tian et al., 2011) that extracellular 10 µM TFP suppresses Ano1 current. If TFP is blocking Ano1 by binding to CaM, one would expect that the site of action of TFP would be intracellular. Because TFP is hydrophobic, it is possible that extracellularly applied TFP crosses the membrane and acts intracellularly. To test this prediction, we applied concentrations of TFP as high as 100 µM to the cytosolic face of inside-out excised patches. No effect of TFP was observed, suggesting that TFP acts at a site that is not accessible to intracellularly applied drug (Fig. 8, D and F). As another test for the involvement of CaM, we tested the effect of a peptide inhibitor of CaM. The peptide corresponds to the high-affinity CaM-binding site on CaMKII (281–309) and would be expected to compete for CaM binding to its targets (Colbran et al., 1989). This peptide does not cause any effect when applied to the cytoplasmic side of excised patches (Fig. 8, E and F).

DISCUSSION

This study provides strong evidence that neither CaM nor Ca^{2+}-stimulated reversible phosphorylation or dephosphorylation is required for the channel to open. Although some of our results are negative and individual experiments alone might not be compelling, the combination of approaches leads to a conclusion that is hard to counter. It should be emphasized that our data do not imply that the channel is not regulated by CaM or by phosphorylation. Our experiments only address the question of whether binding of Ca^{2+} to CaM or Ca^{2+}-stimulated phosphorylation is a requisite step in the opening of the channel by Ca^{2+}. It is entirely possible that that channel is prephosphorylated or that CaM may modulate Ano1 gating in ways not examined here, for example as proposed by Jung et al. (2013). It is also possible that Ano1 can be opened in Ca^{2+}-independent ways (Xiao et al., 2011; Cho et al., 2012).

Regulation of ion channels by tethered versus mobile CaM

Regulation of ion channels by CaM has been shown to occur essentially by two different modes, tethered and mobile (Chin and Means, 2000; Saucerman and Bers, 2012). In the tethered mode, CaM is bound stoichiometrically as a constitutive subunit of the channel independent of Ca^{2+} (class A effector). This has been shown to be the case for SK (Maylie et al., 2004) and Ca_V channels (Mori et al., 2008; Minor and Findeisen, 2010). In the mobile mode, CaM binds to the channel only in its Ca^{2+}-liganded form or regulates the channel indirectly by activating protein kinase or phosphatase cascades. One
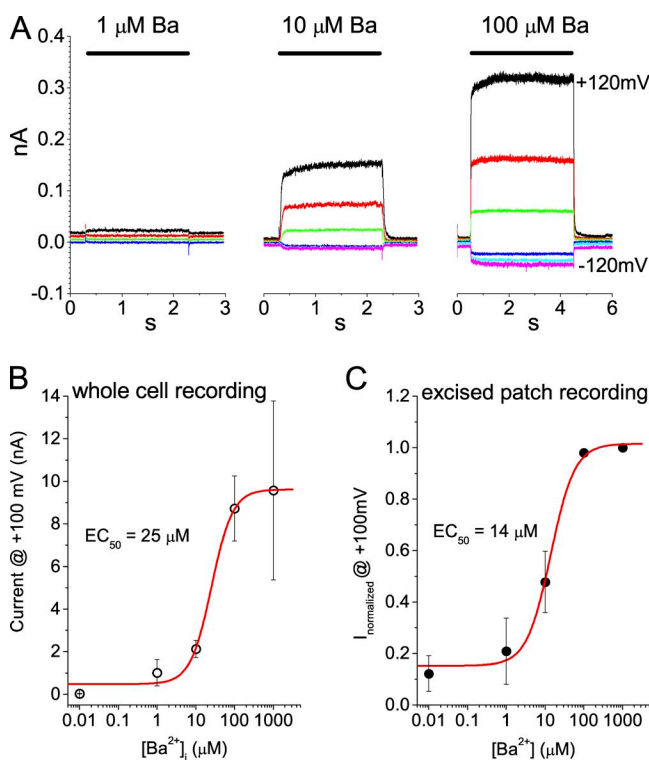

Figure 7. Ano1 is activated by Ba^{2+}. (A) Representative traces of Ano1 current in inside-out excised patches activated by 1, 10, and 100 µM Ba^{2+}. Inside-out excised patches were switched between zero divalent cation (5 mM EGTA with no added Ba^{2+} or Ca^{2+}) and Ba^{2+}-containing pipette solutions. Ba^{2+} solutions contained 1 mM EGTA, and free Ba^{2+} was calculated from MaxChelator. Traces were recorded at the following voltages: black, 120 mV; red, 80 mV; green, 40 mV; blue, −40 mV; cyan, −80 mV; magenta, −120 mV. (B) Mean amplitude of Ba^{2+}-activated current in whole-cell recording at 100 mV. Ba^{2+} was included in the intracellular pipette solution, and current amplitudes were recorded at a time when the currents reached a maximum level. (C) Mean amplitude of Ba^{2+}-activated currents in inside-out excised patches. To control for different current amplitudes between patches and rundown, each patch was exposed for 5-s intervals first to 1 mM Ba^{2+}, then to the test Ba^{2+} concentration, and then to 1 mM Ba^{2+} again. The amplitude of the current in response to the test Ba^{2+} concentration was then normalized to the mean of the currents in 1 mM Ba^{2+}. The data points were fitted to the Hill equation. Error bars are ±SEM.

would expect that if Ano1 was regulated by reversible binding of mobile Ca^{2+}-CaM, the Ca^{2+}-activated current would quickly be lost in excised patches as CaM washed away. Although the Ano1 current ran down in excised patches, it was not restored by addition of exogenous CaM. Our data agree with experiments by Stephan et al. (2009) and Pifferi et al. (2009) on Ano2, a closely related paralogue of Ano1, that show that Ano2 rundown in excised patches cannot be stopped or rescued by addition of CaM, ATP, DTT, cAMP, or vanadate.

We believe that the rate of rundown is much slower than one would expect if CaM were freely diffusible. In vitro stopped-flow experiments have measured the dissociation rates of CaM from CaMKII and from nitric oxide synthase peptides upon switching from a Ca^{2+}- to an EGTA-containing solution to be between 1.6/s and 4.5/s (Byrne et al., 2009; Wu et al., 2011). If the rate of CaM dissociation from Ano1 were similar, one would predict that the Ano1 current would be lost within several seconds of patch excision. However, diffusion of CaM out of the patch is likely slowed by the physical properties (viscosity, for example) of the cortical cytoplasm stuck to the patch. FRAP measurements of the mobility of CaM in the cytoplasm of intact smooth muscle cells show that the mobile CaM fraction has an apparent diffusion coefficient of 0.5 μm^2/s in resting Ca^{2+} and 1 μm^2/s when cytosolic Ca^{2+} is elevated to 0.5–3 μM Ca^{2+} (Luby-Phelps et al., 1995). Because these values are approximately five times slower than diffusion of dextran of the same size, CaM diffusion is indeed slowed by transient binding to immobile binding sites, by tight binding to mobile binding sites, or by the viscosity of the cytoplasm. In any case, the mean displacement (r)

of a particle by diffusion in three dimensions is given by $r = \sqrt{6Dt}$, where D is the diffusion coefficient (1 μm^2/s) and t is time. This equation predicts that in 1 s, mobile CaM would diffuse, on average, 1.7 μm in cytoplasm and would be removed from the patch within seconds in the experiments of Figs. 1 C or 2. The simplest interpretation of these data is that mobile CaM is not involved in Ano1 activation by Ca^{2+}.

If CaM is a tethered subunit of the Ano1 channel that is not freely diffusible, one would expect that overexpression of mutants of CaM that are defective in Ca^{2+} binding would decrease the current, as has been reported for SK channels (Xia et al., 1998). However, we find that $CaM_{2,3,4}$ and $CaM_{1,2,3,4}$ have no effect on Ano1 currents although they significantly decrease SK2 currents. These data are compelling evidence that tethered CaM in not required for Ano1 activation. We cannot rule out the possibility that these mutants are incapable of competing for binding of native CaM to Ano1 even though they are capable of inhibiting SK2 currents. This possibility should be considered in light of recent data from Vocke et al. (2013).

Another piece of datum that indicates that CaM is not required for activation of Ano1 by Ca^{2+} is the ability of Ba^{2+} to activate Ano1 currents. The difference in size between Ba^{2+} and Ca^{2+} generally makes Ba^{2+} a poor substitute for Ca^{2+} in activating CaM (Chao et al., 1984). The inability of Ba^{2+} to substitute for Ca^{2+} has been widely used as a test for CaM involvement in various processes (for example, Proks and Ashcroft, 1995; Gu and Cooper, 2000). A prime example is the almost complete elimination of Ca^{2+}-dependent inactivation of voltage-gated Ca^{2+} channels when Ba^{2+} is the charge carrier (Oliveria et al., 2012).
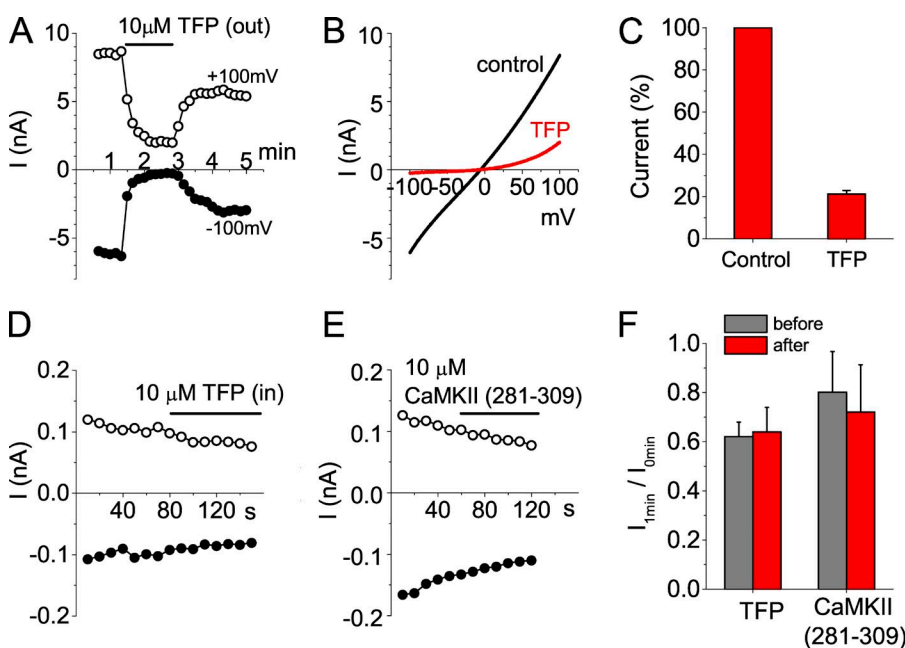

Figure 8. TFP, a CaM inhibitor, inhibits Ano1 in a voltage-dependent manner in whole-cell and excised inside-out patch recordings. (A) Effect of extracellular 10 µM TFP on whole-cell Ano1 current activated by 20 µM Ca^{2+}. TFP inhibits the current, and the effect is partially reversed upon washout. (B) I-V relationship of Ano1 before and 1 min after extracellular application of TFP. (C) The mean normalized currents at 100 mV after 1-min exposure to TFP ($n = 4$). (D) Application of 10 µM TFP to the cytosolic side of an inside-out excised patch has no effect on Ano1 current. (E) A CaM-binding peptide, 10 µM CaMKII (281–309), applied to the cytosolic side of an inside-out patch causes no effect on Ano1 current in inside-out patch. (F) Quantification of the effect of TFP and CaMKII(281–309) on Ano1 current. The current decrease was quantified before and during exposure to compounds as I_{1min}/I_{0min} as described in Fig. 2 ($n = 3$). Error bars are ±SEM.

Kinetics of Ano1 activation

Our results show that Ano1 is activated extremely rapidly by photolysis of caged Ca^{2+}, but these measurements do not distinguish between direct binding of Ca^{2+} to Ano1 and a mechanism involving mobile CaM. SK channels are activated with τ = 6–13 ms in excised patches rapidly perfused with 10 µM Ca^{2+} (Xia et al., 1998). This is slower than the activation rate of Ano1 in response to photolysis of caged Ca^{2+} (τ = 1.2 ms), but is similar to the rate we have observed (τ = 3–6 ms) with fast perfusion under similar conditions. These differences could easily be explained by the mechanics of the fast switching device or by different rates of gating conformational changes after agonist binding.

On the basis of kinetics alone, we cannot exclude an enzymatic activation mechanism of Ano1, as some enzymatic reactions are extremely fast. But a comparison of the kinetics of Ano1 activation to other well-studied ion channels places Ano1 in the same category as ligand-gated channels (Lester et al., 1980). Although protein kinases and protein phosphatases can operate at rates as high as $\sim$30/s in vitro with small substrates under optimal conditions (Adams and Taylor, 1992; Montalibet et al., 2005), the rate of Ano1 current activation is >20 times faster. Likewise, Ano1 activation is 100 times more rapid than the G-protein–gated channel $K_{ir}3$ by agonist (Nargeot et al., 1982), which involves binding of agonist to the receptor, nucleotide exchange, dissociation of G-protein subunits, and association of $\beta\gamma$ subunits with the channel. The observation that Ano1 activation by Ca^{2+} is much faster than activation of $K_{ir}3$ channels is consistent with Ano1 activation requiring fewer or more rapid steps.

In agreement with our data, Tian et al. (2011) conclude that phosphorylation is not required for Ano1 activation. However, despite their finding that elimination of ATP from the internal solution has no effect on Ano1 currents, they conclude that "cytosolic ATP is required for complete activation" of Ano1 because inclusion of the ATP-cleaving enzyme apyrase in the patch pipette completely blocked the current activated by ionomycin or purinergic receptor stimulation. Although their result suggests that ATP is generated endogenously in cells patch-clamped in the whole-cell configuration, our data show that activation of Ano1 in excised patches does not require ATP.

Other studies suggest CaM is involved in CaCC activation

Given our rather strong evidence that Ano1 does not require CaM for activation, how do we explain other studies that show a role for CaM-dependent phosphorylation in activation of a variety of native CaCCs (Nishimoto et al., 1991; Tohda et al., 1991; Wagner et al., 1991; Worrell and Frizzell, 1991; Morris and Frizzell, 1993; Schumann et al., 1993; Chan et al., 1994; Chao et al., 1995; Braun and Schulman, 1996; Xie et al., 1996; Arreola et al., 1998) and suggest that CaM binds to Ano1 (Tian et al., 2011; Jung et al., 2013)? For example, Arreola et al. (1998) concluded that native CaCC currents in parotid gland could be explained by direct Ca^{2+} activation, but that CaCC currents in T84 cells required CaM-dependent phosphorylation. The biophysical properties of the CaM-dependent CaCC currents in many of these studies differ from those of Ano1 currents, so it is possible that these currents are encoded by genes other than Ano1 or that different Ano1 splice variants are involved. The anoctamin gene family consists of 10 members, but it remains uncertain which of these function as plasma membrane Cl^- channels (Martins et al., 2011; Duran et al., 2012; Yang et al., 2012). Four different splice variants of Ano1 have been described and some have different Ca^{2+} sensitivities (Ferrera et al., 2009, 2011; Xiao et al., 2011). For example, the Calmodulin Target Database predicts a CaM-binding site with high probability that overlaps the *d* splice segment located in the loop connecting putative transmembrane domains 2 and 3. The *d* splice segment is not present in the clones studied by us, Tian et al. (2011), and Jung et al. (2013).

Tian et al. (2011) have concluded that there is a CaM-binding site in Ano1(*abc*) that is required for channel activation by Ca^{2+}. This putative CaM-binding site overlaps with the *b* splice segment. One piece of evidence they provide in support of this idea is that the CaM antagonists TFP and J8 inhibit the Ano1 current. We believe that the effect of TFP is not explained by antagonism of CaM because TFP has no effect when applied from the cytosolic side of excised patches at concentrations 10-fold higher than that required to inhibit the current from the outside. Curiously, Vocke et al. (2013) report that TFP and J8 do not inhibit Ano1 currents. The second piece of evidence of Tian et al. (2011) is that inclusion of a peptide corresponding to the putative CaM-binding site in Ano1 in the patch pipette inhibits the Ano1 current in both human and mouse Ano1. It was presumed that the peptide competes for native Ano1 binding to CaM, but no evidence was presented confirming this mode of action, and no positive control with a known CaM-binding peptide was included. We find that the CaM-binding peptide derived from CaMKII(281–309) applied to excised patches has no effect on the Ano1 current. Finally, Tian et al. (2011) show that CaM coimmunoprecipitated with Ano1, but from their figures it appears that the stoichiometric amount of CaM relative to Ano1 is extremely small. Furthermore, it is not shown that deletion of the *b* segment eliminates CaM coimmunoprecipitation. Therefore, we remain skeptical of their conclusion.

Recently, Jung et al. (2013) reported that human Ano1(*ac*) is regulated by CaM but does not require CaM for Ca^{2+}-dependent activation. These investigators show that the relative HCO_3:Cl permeability of the channel increases with cytosolic [Ca^{2+}] and they propose that

this effect is mediated by CaM because silencing all three CaM genes with siRNA eliminates the change in relative anion permeability. They identify two regions that are potential CaM-binding sites. One site ([339]IDLVRKY-F̲GEKVGL̲[352]) is located immediately N-terminal to TM1, and the second site ([772]V̲AIRAKDI̲GIWYNI̲[785]) is located just N-terminal to TM7. The first site receives a high score by the Calmodulin Target Database for being a CaM-binding site, but the score for the second site is extremely low. This low score is achieved because 1-8-14 domains usually have bulky hydrophobic amino acids at the underlined positions, whereas this sequence contains small hydrophobic amino acids. Nevertheless, Jung et al. (2013) show that mutations in either of these domains reduce Ano1 pull-down by CaM-GST and reduce the relative HCO_3^- permeability at high Ca^{2+}. Furthermore, in agreement with our data, these mutations apparently do not affect the ability of Ca^{2+} to activate Ano1.

Very recently, Vocke et al. (2013) showed that $CaM_{1,2}$ and $CaM_{3,4}$ reduce Ano1 current amplitude $\sim$50% but that $CaM_{1,2,3,4}$ has no effect. They also showed that $CaM_{1,2}$ and $CaM_{3,4}$ bind to Ano1 peptides derived from CBM1 but that $CaM_{1,2,3,4}$ did not. These data suggest that $CaM_{1,2}$ and $CaM_{3,4}$ bind to Ano1 and that Ca^{2+} binding to the Ca^{2+}-competent lobe augments Ano1 currents. However, the observation that these mutant CaMs do not completely inhibit the Ano1 current is also consistent with the conclusion that CaM is not required for Ano1 activation by Ca^{2+}.

We reach different conclusions than Tian et al. (2011), Jung et al. (2013), and Vocke et al. (2013) about the physical interaction of CaM with Ano1. Based on three different experiments, we conclude that the interaction of Ano1 with CaM is weak at best. In coimmunoprecipitation experiments (this paper) and mass spectrometric analysis of cross-linked Ano1-binding partners (Perez-Cornejo et al., 2012), we find no evidence of interaction of CaM with Ano1. Both of these experiments measured binding of overexpressed Ano1 to endogenous levels of native CaM. To test whether different methodologies explain the differences between our results and those of Jung et al. (2013), we measured the ability of CaM-GST bound to glutathione–Sepharose beads to capture Ano1 from lysates of Ano1-expressing HEK cells as described by Jung et al. (2013). Although mAno1(ac) hAno1(ac) could be captured by CaM-GST, the fraction of Ano1 that bound to CaM-GST was extremely small compared with the fraction of CaMKIIα that bound. These data suggest that the binding of Ano1 to CaM is small or weak compared with CaMKIIα binding. We conclude that the binding of CaM to Ano1 that is observed in the pull-down assay does not represent the physiological situation. This assay exposes a very small amount of Ano1 to a huge excess of CaM, a condition which would promote the detection of low-affinity interactions. The observation that Ano1 binding is Ca^{2+} dependent does not provide

evidence of specificity because Ca^{2+} causes CaM to change to a conformation that exposes hydrophobic domains that could interact nonspecifically with a hydrophobic protein such as Ano1. Our interpretation is subject to several caveats that we cannot easily test. The fact that CaMKII is a soluble protein and Ano1 is a membrane protein could affect the interaction with CaM-GST. For example, Ano1 may be misfolded in the lysis buffer. Also, different levels of expression of CaMKII and Ano1 could affect the results. We cannot determine the levels of expression with our current methodology because band intensity on Western blots depends not only on protein concentration, but also on the reactivity of the antibodies that are used for detection. Our inability to detect a stable interaction between Ano1 and CaM agrees with the recent study of Terashima et al. (2013) using purified Ano1 and CaM.

The data here strengthen our previous suggestion (Yu et al., 2012) that Ca^{2+} opens the Ano1 channel by directly binding to the pore-forming subunit, Ano1. We have found that mutation of two glutamic acids, E702 and E705, drastically alters the Ca^{2+} sensitivity of the channel. This finding has been confirmed by Terashima et al. (2013) with purified Ano1 incorporated into liposomes, and mutation of the homologous amino acids in Ano6 has the same effect in greatly reducing Ca^{2+} sensitivity (Yang et al., 2012). These data strongly support the conclusion that Ano1 can be gated by direct Ca^{2+} binding in this region of the protein and that CaM is not required, although CaM may possibly modulate Ano1.

It must be emphasized again that our experiments focus on the mechanisms of channel opening by Ca^{2+} and do not directly address the question of whether phosphorylation or CaM can modulate channel function. Ano1 gating is complex and it is entirely possible that the channel is regulated in multiple ways by Ca^{2+}. Some aspects of Ano1 behavior may be mediated by direct Ca binding and others by a separate Ca sensor. This Ca^{2+} sensor could be a Ca^{2+}-binding protein different from CaM. A precedent is provided by Ca_V channels that are regulated both by CaM and members of another family of Ca^{2+}-binding proteins, CaBPs1–4 (Oz et al., 2013). An intriguing property of the Ano1 current is that its waveform and rectification depend on the Ca^{2+} concentration and these different properties might be regulated differentially by different Ca^{2+}-binding sites (Hartzell et al., 2005). At submicromolar Ca^{2+} concentrations, the current strongly outwardly rectifies and activates slowly with depolarization, whereas at higher Ca^{2+} concentrations the Ano1 current exhibits little or no rectification and activates very quickly with depolarization (Xiao et al., 2011). These differing behaviors of Ano1 may support different cellular functions; for example, Ano1 may differentially mediate secretion or absorption of fluid in epithelia or elicit excitation or inhibition in excitable tissues depending on Ca^{2+} concentration (Yu et al., 2012).

Author contributions: K. Yu conceived, designed, and performed experiments, analyzed data, prepared figures, and wrote the manuscript. J. Zhu designed and performed experiments, analyzed data, and prepared figures. Z. Qu designed and performed experiments and analyzed data. Y.-Y. Cui designed and performed experiments and analyzed data. H.C. Hartzell conceived and designed experiments, analyzed data, and wrote the manuscript.

Angus C. Nairn served as editor.

REFERENCES

Adams, J.A., and S.S. Taylor. 1992. Energetic limits of phosphotransfer in the catalytic subunit of cAMP-dependent protein kinase as measured by viscosity experiments. *Biochemistry.* 31:8516–8522. http://dx.doi.org/10.1021/bi00151a019

Arreola, J., J.E. Melvin, and T. Begenisich. 1998. Differences in regulation of Ca^{2+}-activated Cl$^-$ channels in colonic and parotid secretory cells. *Am. J. Physiol. Cell Physiol.* 274:C161–C166.

Braun, A.P., and H. Schulman. 1996. Distinct voltage-dependent gating behaviours of a swelling-activated chloride current in human epithelial cells. *J. Physiol.* 495:743–753.

Britschgi, A., A. Bill, H. Brinkhaus, C. Rothwell, I. Clay, S. Duss, M. Rebhan, P. Raman, C.T. Guy, K. Wetzel, et al. 2013. Calcium-activated chloride channel ANO1 promotes breast cancer progression by activating EGFR and CAMK signaling. *Proc. Natl. Acad. Sci. USA.* 110:E1026–E1034. http://dx.doi.org/10.1073/pnas.1217072110

Bulley, S., Z.P. Neeb, S.K. Burris, J.P. Bannister, C.M. Thomas-Gatewood, W. Jangsangthong, and J.H. Jaggar. 2012. TMEM16A/ANO1 channels contribute to the myogenic response in cerebral arteries. *Circ. Res.* 111:1027–1036. http://dx.doi.org/10.1161/CIRCRESAHA.112.277145

Byrne, M.J., J.A. Putkey, M.N. Waxham, and Y. Kubota. 2009. Dissecting cooperative calmodulin binding to CaM kinase II: a detailed stochastic model. *J. Comput. Neurosci.* 27:621–638. http://dx.doi.org/10.1007/s10827-009-0173-3

Caputo, A., E. Caci, L. Ferrera, N. Pedemonte, C. Barsanti, E. Sondo, U. Pfeffer, R. Ravazzolo, O. Zegarra-Moran, and L.J.V. Galietta. 2008. TMEM16A, a membrane protein associated with calcium-dependent chloride channel activity. *Science.* 322:590–594. http://dx.doi.org/10.1126/science.1163518

Chan, H.C., M.A. Kaetzel, A.L. Gotter, J.R. Dedman, and D.J. Nelson. 1994. Annexin IV inhibits calmodulin-dependent protein kinase II-activated chloride conductance. A novel mechanism for ion channel regulation. *J. Biol. Chem.* 269:32464–32468.

Chao, A.C., K. Kouyama, E.K. Heist, Y.J. Dong, and P. Gardner. 1995. Calcium- and CaMKII-dependent chloride secretion induced by the microsomal Ca(2+)-ATPase inhibitor 2,5-di-(tert-butyl)-1,4-hydroquinone in cystic fibrosis pancreatic epithelial cells. *J. Clin. Invest.* 96:1794–1801. http://dx.doi.org/10.1172/JCI118225

Chao, S.H., Y. Suzuki, J.R. Zysk, and W.Y. Cheung. 1984. Activation of calmodulin by various metal cations as a function of ionic radius. *Mol. Pharmacol.* 26:75–82.

Chin, D., and A.R. Means. 2000. Calmodulin: a prototypical calcium sensor. *Trends Cell Biol.* 10:322–328. http://dx.doi.org/10.1016/S0962-8924(00)01800-6

Cho, H., Y.D. Yang, J. Lee, B. Lee, T. Kim, Y. Jang, S.K. Back, H.S. Na, B.D. Harfe, F. Wang, et al. 2012. The calcium-activated chloride channel anoctamin 1 acts as a heat sensor in nociceptive neurons. *Nat. Neurosci.* 15:1015–1021. http://dx.doi.org/10.1038/nn.3111

Colbran, R.J., M.K. Smith, C.M. Schworer, Y.L. Fong, and T.R. Soderling. 1989. Regulatory domain of calcium/calmodulin-dependent protein kinase II. Mechanism of inhibition and regulation by phosphorylation. *J. Biol. Chem.* 264:4800–4804.

Cole, W.C. 2011. ANO1-ther brick in the wall—role of Ca2+-activated Cl- channels of interstitial cells of Cajal in cholinergic motor control of gastrointestinal smooth muscle. *J. Physiol.* 589:4641–4642. http://dx.doi.org/10.1113/jphysiol.2011.218453

Davis, A.J., A.S. Forrest, T.A. Jepps, M.L. Valencik, M. Wiwchar, C.A. Singer, W.R. Sones, I.A. Greenwood, and N. Leblanc. 2010. Expression profile and protein translation of TMEM16A in murine smooth muscle. *Am. J. Physiol. Cell Physiol.* 299:C948–C959. http://dx.doi.org/10.1152/ajpcell.00018.2010

Davis, A.J., J. Shi, H.A. Pritchard, P.S. Chadha, N. Leblanc, G. Vasilikostas, Z. Yao, A.S. Verkman, A.P. Albert, and I.A. Greenwood. 2013. Potent vasorelaxant activity of the TMEM16A inhibitor T16A(inh) -A01. *Br. J. Pharmacol.* 168:773–784. http://dx.doi.org/10.1111/j.1476-5381.2012.02199.x

Dixon, R.E., G.W. Hennig, S.A. Baker, F.C. Britton, B.D. Harfe, J.R. Rock, K.M. Sanders, and S.M. Ward. 2012. Electrical slow waves in the mouse oviduct are dependent upon a calcium activated chloride conductance encoded by Tmem16a. *Biol. Reprod.* 86:1–7. http://dx.doi.org/10.1095/biolreprod.111.095554

Duran, C., Z. Qu, A.O. Osunkoya, Y. Cui, and H.C. Hartzell. 2012. ANOs 3-7 in the anoctamin/Tmem16 Cl- channel family are intracellular proteins. *Am. J. Physiol. Cell Physiol.* 302:C482–C493. http://dx.doi.org/10.1152/ajpcell.00140.2011

Dutta, A.K., A.K. Khimji, C. Kresge, A. Bugde, M. Dougherty, V. Esser, Y. Ueno, S.S. Glaser, G. Alpini, D.C. Rockey, and A.P. Feranchak. 2011. Identification and functional characterization of TMEM16A, a Ca2+-activated Cl- channel activated by extracellular nucleotides, in biliary epithelium. *J. Biol. Chem.* 286:766–776. http://dx.doi.org/10.1074/jbc.M110.164970

Duvvuri, U., D.J. Shiwarski, D. Xiao, C. Bertrand, X. Huang, R.S. Edinger, J.R. Rock, B.D. Harfe, B.J. Henson, K. Kunzelmann, et al. 2012. TMEM16A induces MAPK and contributes directly to tumorigenesis and cancer progression. *Cancer Res.* 72:3270–3281. http://dx.doi.org/10.1158/0008-5472.CAN-12-0475-T

Ellis-Davies, G.C., and R.J. Barsotti. 2006. Tuning caged calcium: photolabile analogues of EGTA with improved optical and chelation properties. *Cell Calcium.* 39:75–83. http://dx.doi.org/10.1016/j.ceca.2005.10.003

Ellis-Davies, G.C., and J.H. Kaplan. 1994. Nitrophenyl-EGTA, a photolabile chelator that selectively binds Ca^{2+} with high affinity and releases it rapidly upon photolysis. *Proc. Natl. Acad. Sci. USA.* 91:187–191. http://dx.doi.org/10.1073/pnas.91.1.187

Ellis-Davies, G.C., J.H. Kaplan, and R.J. Barsotti. 1996. Laser photolysis of caged calcium: rates of calcium release by nitrophenyl-EGTA and DM-nitrophen. *Biophys. J.* 70:1006–1016. http://dx.doi.org/10.1016/S0006-3495(96)79644-3

Erickson, M.G., B.A. Alseikhan, B.Z. Peterson, and D.T. Yue. 2001. Preassociation of calmodulin with voltage-gated Ca(2+) channels revealed by FRET in single living cells. *Neuron.* 31:973–985. http://dx.doi.org/10.1016/S0896-6273(01)00438-X

Ferrera, L., A. Caputo, I. Ubby, E. Bussani, O. Zegarra-Moran, R. Ravazzolo, F. Pagani, and L.J. Galietta. 2009. Regulation of TMEM16A chloride channel properties by alternative splicing.

J. Biol. Chem. 284:33360–33368. http://dx.doi.org/10.1074/jbc.M109.046607

Ferrera, L., P. Scudieri, E. Sondo, A. Caputo, E. Caci, O. Zegarra-Moran, R. Ravazzolo, and L.J. Galietta. 2011. A minimal isoform of the TMEM16A protein associated with chloride channel activity. *Biochim. Biophys. Acta.* 1808:2214–2223. http://dx.doi.org/10.1016/j.bbamem.2011.05.017

Frace, A.M., P.F. Méry, R. Fischmeister, and H.C. Hartzell. 1993. Rate-limiting steps in the beta-adrenergic stimulation of cardiac calcium current. *J. Gen. Physiol.* 101:337–353. http://dx.doi.org/10.1085/jgp.101.3.337

Geiser, J.R., D. van Tuinen, S.E. Brockerhoff, M.M. Neff, and T.N. Davis. 1991. Can calmodulin function without binding calcium? *Cell.* 65:949–959. http://dx.doi.org/10.1016/0092-8674(91)90547-C

Gu, C., and D.M. Cooper. 2000. Ca(2+), Sr(2+), and Ba(2+) identify distinct regulatory sites on adenylyl cyclase (AC) types VI and VIII and consolidate the apposition of capacitative cation entry channels and Ca(2+)-sensitive ACs. *J. Biol. Chem.* 275:6980–6986. http://dx.doi.org/10.1074/jbc.275.10.6980

Hartzell, C., I. Putzier, and J. Arreola. 2005. Calcium-activated chloride channels. *Annu. Rev. Physiol.* 67:719–758. http://dx.doi.org/10.1146/annurev.physiol.67.032003.154341

Hidalgo, A.A., W. Caetano, M. Tabak, and O.N. Oliveira Jr. 2004. Interaction of two phenothiazine derivatives with phospholipid monolayers. *Biophys. Chem.* 109:85–104. http://dx.doi.org/10.1016/j.bpc.2003.10.020

Huang, F., H. Zhang, M. Wu, H. Yang, M. Kudo, C.J. Peters, P.G. Woodruff, O.D. Solberg, M.L. Donne, X. Huang, et al. 2012. Calcium-activated chloride channel TMEM16A modulates mucin secretion and airway smooth muscle contraction. *Proc. Natl. Acad. Sci. USA.* 109:16354–16359. http://dx.doi.org/10.1073/pnas.1214596109

Huang, X., D. Zhao, Z.Y. Wang, M.L. Zhang, Z.Q. Yan, Y.F. Han, W.X. Xu, and Z.L. Jiang. 2010. The properties of spontaneous transient inward currents of interstitial cells in rabbit portal vein. *Eur. J. Pharmacol.* 643:63–69. http://dx.doi.org/10.1016/j.ejphar.2010.06.011

Ikemoto, Y., A. Yoshida, and M. Oda. 1992. Blockade by trifluoperazine of a Ca(2+)-activated K+ channel in rat hippocampal pyramidal neurons. *Eur. J. Pharmacol.* 216:191–198. http://dx.doi.org/10.1016/0014-2999(92)90360-G

Jung, J., J.H. Nam, H.W. Park, U. Oh, J.H. Yoon, and M.G. Lee. 2013. Dynamic modulation of ANO1/TMEM16A HCO3(-) permeability by Ca2+/calmodulin. *Proc. Natl. Acad. Sci. USA.* 110:360–365. http://dx.doi.org/10.1073/pnas.1211594110

Kuruma, A., and H.C. Hartzell. 2000. Bimodal control of a Ca^{2+}-activated Cl^{-} channel by different Ca^{2+} signals. *J. Gen. Physiol.* 115:59–80. http://dx.doi.org/10.1085/jgp.115.1.59

Lester, H.A., M.M. Nass, M.E. Krouse, J.M. Nerbonne, N.H. Wassermann, and B.F. Erlanger. 1980. Electrophysiological experiments with photoisomerizable cholinergic compounds: review and progress report. *Ann. N. Y. Acad. Sci.* 346:475–490. http://dx.doi.org/10.1111/j.1749-6632.1980.tb22118.x

Liu, B., J.E. Linley, X. Du, X. Zhang, L. Ooi, H. Zhang, and N. Gamper. 2010. The acute nociceptive signals induced by bradykinin in rat sensory neurons are mediated by inhibition of M-type K^{+} channels and activation of Ca^{2+}-activated Cl^{-} channels. *J. Clin. Invest.* 120:1240–1252. http://dx.doi.org/10.1172/JCI41084

Luby-Phelps, K., M. Hori, J.M. Phelps, and D. Won. 1995. Ca(2+)-regulated dynamic compartmentalization of calmodulin in living smooth muscle cells. *J. Biol. Chem.* 270:21532–21538. http://dx.doi.org/10.1074/jbc.270.37.21532

Manoury, B., A. Tamuleviciute, and P. Tammaro. 2010. TMEM16A/anoctamin 1 protein mediates calcium-activated chloride currents in pulmonary arterial smooth muscle cells. *J. Physiol.* 588:2305–2314. http://dx.doi.org/10.1113/jphysiol.2010.189506

Martins, J.R., D. Faria, P. Kongsuphol, B. Reisch, R. Schreiber, and K. Kunzelmann. 2011. Anoctamin 6 is an essential component of the outwardly rectifying chloride channel. *Proc. Natl. Acad. Sci. USA.* 108:18168–18172. http://dx.doi.org/10.1073/pnas.1108094108

Maylie, J., C.T. Bond, P.S. Herson, W.S. Lee, and J.P. Adelman. 2004. Small conductance Ca2+-activated K+ channels and calmodulin. *J. Physiol.* 554:255–261. http://dx.doi.org/10.1113/jphysiol.2003.049072

Mazzone, A., S.T. Eisenman, P.R. Strege, Z. Yao, T. Ordog, S.J. Gibbons, and G. Farrugia. 2012. Inhibition of cell proliferation by a selective inhibitor of the Ca(2+)-activated Cl(-) channel, Ano1. *Biochem. Biophys. Res. Commun.* 427:248–253. http://dx.doi.org/10.1016/j.bbrc.2012.09.022

McCann, J.D., and M.J. Welsh. 1987. Neuroleptics antagonize a calcium-activated potassium channel in airway smooth muscle. *J. Gen. Physiol.* 89:339–352. http://dx.doi.org/10.1085/jgp.89.2.339

Minor, D.L. Jr., and F. Findeisen. 2010. Progress in the structural understanding of voltage-gated calcium channel (CaV) function and modulation. *Channels (Austin).* 4:459–474.

Montalibet, J., K.I. Skorey, and B.P. Kennedy. 2005. Protein tyrosine phosphatase: enzymatic assays. *Methods.* 35:2–8. http://dx.doi.org/10.1016/j.ymeth.2004.07.002

Mori, M.X., C.W. Vander Kooi, D.J. Leahy, and D.T. Yue. 2008. Crystal structure of the CaV2 IQ domain in complex with Ca2+/calmodulin: high-resolution mechanistic implications for channel regulation by Ca2+. *Structure.* 16:607–620. http://dx.doi.org/10.1016/j.str.2008.01.011

Morris, A.P., and R.A. Frizzell. 1993. Ca(2+)-dependent Cl- channels in undifferentiated human colonic cells (HT-29). II. Regulation and rundown. *Am. J. Physiol.* 264:C977–C985.

Mullins, F.M., C.Y. Park, R.E. Dolmetsch, and R.S. Lewis. 2009. STIM1 and calmodulin interact with Orai1 to induce Ca2+-dependent inactivation of CRAC channels. *Proc. Natl. Acad. Sci. USA.* 106:15495–15500. http://dx.doi.org/10.1073/pnas.0906781106

Nargeot, J., H.A. Lester, N.J. Birdsall, J. Stockton, N.H. Wassermann, and B.F. Erlanger. 1982. A photoisomerizable muscarinic antagonist. Studies of binding and of conductance relaxations in frog heart. *J. Gen. Physiol.* 79:657–678. http://dx.doi.org/10.1085/jgp.79.4.657

Nishimoto, I., J.A. Wagner, H. Schulman, and P. Gardner. 1991. Regulation of Cl- channels by multifunctional CaM kinase. *Neuron.* 6:547–555. http://dx.doi.org/10.1016/0896-6273(91)90057-7

Oliveria, S.F., P.J. Dittmer, D.H. Youn, M.L. Dell'Acqua, and W.A. Sather. 2012. Localized calcineurin confers Ca2+-dependent inactivation on neuronal L-type Ca2+ channels. *J. Neurosci.* 32:15328–15337. http://dx.doi.org/10.1523/JNEUROSCI.2302-12.2012

Orta, G., G. Ferreira, O. José, C.L. Treviño, C. Beltrán, and A. Darszon. 2012. Human spermatozoa possess a calcium-dependent chloride channel that may participate in the acrosomal reaction. *J. Physiol.* 590:2659–2675. http://dx.doi.org/10.1113/jphysiol.2011.224485

Ousingsawat, J., J.R. Martins, R. Schreiber, J.R. Rock, B.D. Harfe, and K. Kunzelmann. 2009. Loss of TMEM16A causes a defect in epithelial Ca^{2+}-dependent chloride transport. *J. Biol. Chem.* 284:28698–28703. http://dx.doi.org/10.1074/jbc.M109.012120

Oz, S., A. Benmocha, Y. Sasson, D. Sachyani, L. Almagor, A. Lee, J.A. Hirsch, and N. Dascal. 2013. Competitive and non-competitive regulation of calcium-dependent inactivation in CaV1.2 L-type Ca2+ channels by calmodulin and Ca2+-binding protein 1. *J. Biol. Chem.* 288:12680–12691. http://dx.doi.org/10.1074/jbc.M113.460949

Patton, C., S. Thompson, and D. Epel. 2004. Some precautions in using chelators to buffer metals in biological solutions. *Cell Calcium.* 35:427–431. http://dx.doi.org/10.1016/j.ceca.2003.10.006

Perez-Cornejo, P., A. Gokhale, C. Duran, Y. Cui, Q. Xiao, H.C. Hartzell, and V. Faundez. 2012. Anoctamin 1 (Tmem16A) Ca2+-activated chloride channel stoichiometrically interacts

with an ezrin-radixin-moesin network. *Proc. Natl. Acad. Sci. USA.* 109:10376–10381. http://dx.doi.org/10.1073/pnas.1200174109

Peterson, B.Z., C.D. DeMaria, J.P. Adelman, and D.T. Yue. 1999. Calmodulin is the Ca2+ sensor for Ca2+ -dependent inactivation of L-type calcium channels. *Neuron.* 22:549–558 (erratum appears in *Neuron.* 1999. 22:following 893). http://dx.doi.org/10.1016/S0896-6273(00)80709-6

Pifferi, S., M. Dibattista, and A. Menini. 2009. TMEM16B induces chloride currents activated by calcium in mammalian cells. *Pflugers Arch.* 458:1023–1038. http://dx.doi.org/10.1007/s00424-009-0684-9

Proks, P., and F.M. Ashcroft. 1995. Effects of divalent cations on exocytosis and endocytosis from single mouse pancreatic beta-cells. *J. Physiol.* 487:465–477.

Rapp, G., and K. Güth. 1988. A low cost high intensity flash device for photolysis experiments. *Pflugers Arch.* 411:200–203. http://dx.doi.org/10.1007/BF00582315

Rhoads, A.R., and F. Friedberg. 1997. Sequence motifs for calmodulin recognition. *FASEB J.* 11:331–340.

Rock, J.R., W.K. O'Neal, S.E. Gabriel, S.H. Randell, B.D. Harfe, R.C. Boucher, and B.R. Grubb. 2009. Transmembrane protein 16A (TMEM16A) is a Ca^{2+}-regulated Cl^{-} secretory channel in mouse airways. *J. Biol. Chem.* 284:14875–14880. http://dx.doi.org/10.1074/jbc.C109.000869

Romanenko, V.G., M.A. Catalán, D.A. Brown, I. Putzier, H.C. Hartzell, A.D. Marmorstein, M. Gonzalez-Begne, J.R. Rock, B.D. Harfe, and J.E. Melvin. 2010. Tmem16A encodes the Ca^{2+}-activated Cl^{-} channel in mouse submandibular salivary gland acinar cells. *J. Biol. Chem.* 285:12990–13001. http://dx.doi.org/10.1074/jbc.M109.068544

Ruiz, C., J.R. Martins, F. Rudin, S. Schneider, T. Dietsche, C.A. Fischer, L. Tornillo, L.M. Terracciano, R. Schreiber, L. Bubendorf, and K. Kunzelmann. 2012. Enhanced expression of ANO1 in head and neck squamous cell carcinoma causes cell migration and correlates with poor prognosis. *PLoS ONE.* 7:e43265. http://dx.doi.org/10.1371/journal.pone.0043265

Saucerman, J.J., and D.M. Bers. 2012. Calmodulin binding proteins provide domains of local Ca2+ signaling in cardiac myocytes. *J. Mol. Cell. Cardiol.* 52:312–316. http://dx.doi.org/10.1016/j.yjmcc.2011.06.005

Schroeder, B.C., T. Cheng, Y.N. Jan, and L.Y. Jan. 2008. Expression cloning of TMEM16A as a calcium-activated chloride channel subunit. *Cell.* 134:1019–1029. http://dx.doi.org/10.1016/j.cell.2008.09.003

Schumann, M.A., P. Gardner, and T.A. Raffin. 1993. Recombinant human tumor necrosis factor alpha induces calcium oscillation and calcium-activated chloride current in human neutrophils. The role of calcium/calmodulin-dependent protein kinase. *J. Biol. Chem.* 268:2134–2140.

Stephan, A.B., E.Y. Shum, S. Hirsh, K.D. Cygnar, J. Reisert, and H. Zhao. 2009. ANO2 is the cilial calcium-activated chloride channel that may mediate olfactory amplification. *Proc. Natl. Acad. Sci. USA.* 106:11776–11781. http://dx.doi.org/10.1073/pnas.0903304106

Terashima, H., A. Picollo, and A. Accardi. 2013. Purified TMEM16A is sufficient to form Ca2+-activated Cl- channels. *Proc. Natl. Acad. Sci. USA.* 110:19354–19359. http://dx.doi.org/10.1073/pnas.1312014110

Thaler, C., S.V. Koushik, H.L. Puhl III, P.S. Blank, and S.S. Vogel. 2009. Structural rearrangement of CaMKIIalpha catalytic domains encodes activation. *Proc. Natl. Acad. Sci. USA.* 106:6369–6374. http://dx.doi.org/10.1073/pnas.0901913106

Thomas-Gatewood, C., Z.P. Neeb, S. Bulley, A. Adebiyi, J.P. Bannister, M.D. Leo, and J.H. Jaggar. 2011. TMEM16A channels generate Ca^{2+}-activated Cl^{-} currents in cerebral artery smooth muscle cells. *Am. J. Physiol. Heart Circ. Physiol.* 301:H1819–H1827. http://dx.doi.org/10.1152/ajpheart.00404.2011

Tian, Y., P. Kongsuphol, M. Hug, J. Ousingsawat, R. Witzgall, R. Schreiber, and K. Kunzelmann. 2011. Calmodulin-dependent activation of the epithelial calcium-dependent chloride channel TMEM16A. *FASEB J.* 25:1058–1068. http://dx.doi.org/10.1096/fj.10-166884

Tohda, M., J. Nakamura, H. Hidaka, and Y. Nomura. 1991. Inhibitory effects of KN-62, a specific inhibitor of Ca/calmodulin-dependent protein kinase II, on serotonin-evoked C1-current and 36-C1-efflux in *Xenopus* oocytes. *Neurosci. Lett.* 129:47–50. http://dx.doi.org/10.1016/0304-3940(91)90717-8

Vocke, K., K. Dauner, A. Hahn, A. Ulbrich, J. Broecker, S. Keller, S. Frings, and F. Möhrlen. 2013. Calmodulin-dependent activation and inactivation of anoctamin calcium-gated chloride channels. *J. Gen. Physiol.* 142:381–404. http://dx.doi.org/10.1085/jgp.201311015

Wagner, J.A., A.L. Cozens, H. Schulman, D.C. Gruenert, L. Stryer, and P. Gardner. 1991. Activation of chloride channels in normal and cystic fibrosis airway epithelial cells by multifunctional calcium/calmodulin-dependent protein kinase. *Nature.* 349:793–796. http://dx.doi.org/10.1038/349793a0

Worrell, R.T., and R.A. Frizzell. 1991. CaMKII mediates stimulation of chloride conductance by calcium in T84 cells. *Am. J. Physiol.* 260:C877–C882.

Wu, G., V. Berka, and A.-L. Tsai. 2011. Binding kinetics of calmodulin with target peptides of three nitric oxide synthase isozymes. *J. Inorg. Biochem.* 105:1226–1237. http://dx.doi.org/10.1016/j.jinorgbio.2011.06.003

Xia, X.M., B. Fakler, A. Rivard, G. Wayman, T. Johnson-Pais, J.E. Keen, T. Ishii, B. Hirschberg, C.T. Bond, S. Lutsenko, et al. 1998. Mechanism of calcium gating in small-conductance calcium-activated potassium channels. *Nature.* 395:503–507. http://dx.doi.org/10.1038/26758

Xiao, Q., K. Yu, P. Perez-Cornejo, Y. Cui, J. Arreola, and H.C. Hartzell. 2011. Voltage- and calcium-dependent gating of TMEM16A/Ano1 chloride channels are physically coupled by the first intracellular loop. *Proc. Natl. Acad. Sci. USA.* 108:8891–8896. http://dx.doi.org/10.1073/pnas.1102147108

Xie, W., M.A. Kaetzel, K.S. Bruzik, J.R. Dedman, S.B. Shears, and D.J. Nelson. 1996. Inositol 3,4,5,6-tetrakisphosphate inhibits the calmodulin-dependent protein kinase II-activated chloride conductance in T84 colonic epithelial cells. *J. Biol. Chem.* 271:14092–14097. http://dx.doi.org/10.1074/jbc.271.24.14092

Yang, H., A. Kim, T. David, D. Palmer, T. Jin, J. Tien, F. Huang, T. Cheng, S.R. Coughlin, Y.N. Jan, and L.Y. Jan. 2012. TMEM16F forms a Ca2+-activated cation channel required for lipid scrambling in platelets during blood coagulation. *Cell.* 151:111–122. http://dx.doi.org/10.1016/j.cell.2012.07.036

Yang, Y.D., H. Cho, J.Y. Koo, M.H. Tak, Y. Cho, W.S. Shim, S.P. Park, J. Lee, B. Lee, B.M. Kim, et al. 2008. TMEM16A confers receptor-activated calcium-dependent chloride conductance. *Nature.* 455:1210–1215. http://dx.doi.org/10.1038/nature07313

Yu, K., C. Duran, Z. Qu, Y.Y. Cui, and H.C. Hartzell. 2012. Explaining calcium-dependent gating of anoctamin-1 chloride channels requires a revised topology. *Circ. Res.* 110:990–999. http://dx.doi.org/10.1161/CIRCRESAHA.112.264440

Zhu, M.H., T.W. Kim, S. Ro, W. Yan, S.M. Ward, S.D. Koh, and K.M. Sanders. 2009. A Ca(2+)-activated Cl(-) conductance in interstitial cells of Cajal linked to slow wave currents and pacemaker activity. *J. Physiol.* 587:4905–4918. http://dx.doi.org/10.1113/jphysiol.2009.176206